An Intriguing Oscillating Combustion Phenomenon

Justine M. L. Corbel^{1, 2}, Joost N. J. Lingen², John. F. Zevenbergen², Onno L. J. Gijzeman¹, Andries Meijerink¹.

Abstract:

Strobes are pyrotechnic compositions that emit bright flashes of white or colored light at regular time intervals. The strobe effect has applications in various fields, most notably in the fireworks industry and in the military area (signaling – missile decoys – crowd control). However, the chemical and physical mechanisms involved in this curious combustion phenomenon remain unknown. This study investigates parameters that influence the strobe effect (frequency, sharpness of flashes). Variations were applied to the fuel particle size and weight fraction of the ternary composition ammonium perchlorate, magnalium (fuel) and barium sulfate. Both parameters are related to the heat generation and transfer within the composition. The light emission was recorded with photodiodes and a high speed camera (5000 fps). The experimental results served as input for a model to explain the strobe behavior based on layer-by-layer combustion. Moreover, it was established that the flash frequency is dependent on a delicate balance between heat generation in one layer and heat transfer to a next layer. The model gives new insights into the behavior of pyrotechnic strobes and enables a better control of the flash frequency by variation of the size and content of the metal fuel particles.

1. Introduction

A strobe is a pyrotechnic composition which, when ignited, exhibits oscillatory combustion and produces bright flashes of white or colored light while burning. The strobe effect has applications in various fields, most notably in the fireworks industry and in the military area. The application in fireworks is well known to the public as strobe pots or twinklers. In the military, applications involve signaling or missile decoy (1-4). Strobes can also be used for crowd control where an accurate control of the frequency, regularity and sharpness of flashes is important: a frequency of 12 Hz is known to disturb the human visual sensory system most and even may cause an epileptic crisis (5). A better understanding of the chemical and physical mechanisms involved in the curious combustion reaction can help to improve frequency control.

The first known study of strobe compositions dates to an 1898 fireworks historical handbook from Brocks Fireworks Ltd (6). Subsequent compositions showing oscillatory flashing behavior were discovered by trial and error. Systematic strobe mechanism studies started in the 1970s when Krone and Wasmann hypothesized two reactions (a dark and a flash reaction) that alternate at regular intervals (7, 8). Shimizu expanded this hypothesis by identifying fuels and oxidizers for both reactions (9). Later studies showed there cannot be both dark and flash reagents for some simple strobes, suggesting that another mechanism must be operative (10). A thermokinetic model was suggested based on models developed for SHS (Self-propagating High-temperature Synthesis) combustion (11-13). This type of solid-phase combustion is similar to strobe reactions in both the ingredients used as well as intermittent burning behavior (14-21). Here a more detailed model explaining oscillatory combustion of strobes is described with experimental data supporting the theory. The model quantitatively explains the variation in flash frequency as a function of the size and weight fraction of the magnalium particles in the strobe composition.

2. Experimental

¹ Condensed Matter and Interfaces, Faculty of Science, Utrecht University, P.O. Box 80.000, 3508 TA Utrecht, The Netherlands.

² TNO Technical Sciences, Department Energetic Materials, P.O. Box 45, 2250 AA Rijswijk, The Netherlands.

1.1. Compositions:

The effect of particle size and fuel:oxidizer: metal salt ratio is studied. The mixtures are based on a classical strobe composition described in Table 1 (9, 10). Ammonium perchlorate serves as oxidizer while magnalium is the fuel.

Composition (percentage by weight)					
Ammonium		60	57.1	47.6	
perchlorate					
Barium sulfate		17	16.2	13.5	
Magnalium		23	21.9	18.2	
Potassium dichromate		5	4.8	4	
		(additional)			
Binder	Nitrocellulose			16.7	1.7
	Acetone	20	20		15
		(additional)	(additional)		

Table 1: Base compositions of strobes used for this study

The magnalium used is 50:50 magnesium-aluminum alloy from ECKA Granules, Metal powder technologies (Austria). The powder is manufactured from aluminum and magnesium primary metals and they are granulated by mechanical grinding. The grade of the powder is < 100 μ m. The magnalium powder was sieved in five different fractions (38 μ m; 53 μ m; 63 μ m; 75 μ m, 90 μ m) so that narrow particle size distributions were achieved. Six samples of magnalium were obtained and were named magnalium samples 1 to 6. The average determined particle sizes are 24.9 μ m, 41.3 μ m, 58.8 μ m, 60.3 μ m and 96.5 μ m and 114.5 (the determination of the particle size distribution is described in the section *Evaluation of the particle size distribution*). Six compositions were made according to Table 1 with the different magnalium samples.

Nine other compositions were made based on the composition described in Table 1 with a variation of the amount of magnalium. They are listed in Table 2 and in the ternary diagram in Figure 1. The base composition was called composition 2.0. The magnalium sample used is sample 2 (average particle size: $41.3 \mu m$).

Compositions	Ammonium perchlorate	Barium sulfate	Magnalium	Total
2.0	60,0	17,0	23,0	100,0
	60,0	17,0	10,0	87,0
2.1	69,0	19,5	11,5	100,0
	60,0	17,0	15,0	92,0
2.2	65,2	18,5	16,3	100,0
	60,0	17,0	20,0	97,0
2.3	61,9	17,5	20,6	100,0
	60,0	17,0	25,0	102,0
2.4	58,8	16,7	24,5	100,0
	60,0	17,0	30,0	107,0
2.5	56,1	15,9	28,0	100,0
	60,0	17,0	35,0	112,0
2.6	53,6	15,2	31,3	100,0
	60,0	17,0	40,0	117,0
2.7	51,3	14,5	34,2	100,0
	60,0	17,0	45,0	122,0
2.8	49,2	13,9	36,9	100,0

Table 2: Compositions of the strobes used to investigate the influence of the fuel (magnalium) content on the strobe frequency. All numbers refer to weight ratios. The ratio between the oxidizer (ammonium perchlorate) and fuel (magnalium) was varied between 60:10 and 60:45.

Ten grams of each composition were prepared, including a binder solution composed of 10% nitrocellulose and 90% acetone. After mixing, the compositions were pressed (100 bars) into pellets of 1.5 g and then dried into a vacuum oven during two hours. The final average pellet weight of the pellet was 1.26 g; the diameter was 0.99 cm; the average height of the pellets was 0.92 cm; the average density was 0.446 g/cm³. The pellets were placed on a metal plate and ignited with a butane burner. A set of three pellets was ignited for each experiment.

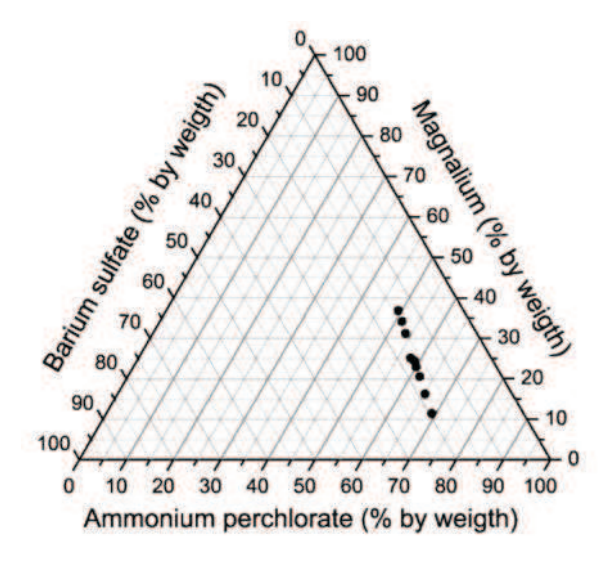


Figure 1: Ternary diagram showing the compositions of Table 2 for studies on the influence of the magnalium content.

1.2. Optical equipment

Movies were recorded with a High-Speed camera (Redlake digital imaging system, 5000 and 3000 frames per second, resolution: 160×160) to follow the light emission of the strobes and to visualize the processes during the dark and the light reactions.

The light emission and the flash frequencies were recorded using photodiodes coupled with an oscilloscope (Sigma 30 from Nicolet technologies). The time resolution was varied from 0.1 to 0.5 ms depending on the frequency of the flashes. Four different types of photodiodes from Roithner Lasertechnik GmbH were used, sensitive in different spectral regions (blue -470 nm; green -525 nm; red -660 nm; infrared -740 nm). No significant differences were observed in the time response of the photodiodes.

1.3. Evaluation of the particle size

The particle size distribution of each sample was recorded with a particle sizer of the Malvern 2600 series that relies on the laser light scattering technique. Three different range lenses were used to obtain the most accurate results; a 100 mm lens for magnalium samples 1 and 2; a 300 mm lens for magnalium samples 3, 4 and 5 and a 600 mm lens for magnalium sample 6. The mathematical model used to analyze the results is based on a Log Normal model. The particle size distribution was measured of two different samples from each magnalium sample. The results are presented in Table 3. D(v, 0.1), D(v, 0.5) and D(v, 0.9) are respectively the diameters (particle size) at 10%, 50% and 90% point of the distribution. The span gives a measure of the width of the volume distribution relative to the median diameter, D(v, 0.5) and is calculated from the percentiles using:

Span =
$$\frac{D(v,0.9) - D(v,0.1)}{D(v,0.5)}$$
 Eq. 1

The values displayed in Table 3 are the averages of the values obtained from the two measurement series. The parameters used further in this study to correlate the strobe frequency to the particle size are the median value D(v, 0.5). Figure 2 shows the size distribution for one of each of the magnalium samples. Note that particle sizes 3 and 4 are very close and who has the largest particle size depends on the parameter chosen to characterize particle size. The size distribution for sample 4 is larger than for sample 3.

Particle size distribution (mean values)	D(v, 0.1) [μm]	D(v, 0.5) [μm]	D(v, 0.9) [µm]	Span	Average particle size [µm]
Magnalium sample 1	10.45	23.89	40.20	1.24	24,85
Magnalium sample 2	15.66	42.50	63.46	1.12	41,29
Magnalium sample 3	26.60	60.69	70.92	0.73	58,82
Magnalium sample 4	25.15	62.67	89.80	1.03	60,31
Magnalium sample 5	68.75	93.75	128.73	0.64	96,50
Magnalium sample 6	88.18	111.88	147.83	0.533	114.52

Table 3: Particle sizes and size distribution for the five samples of magnalium determined with the Malvern 2600.

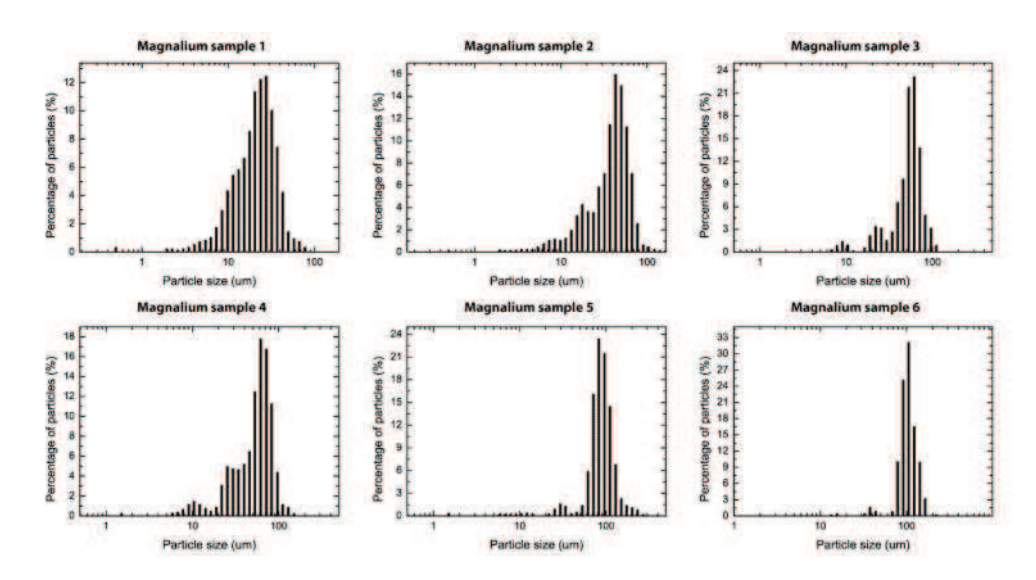


Figure 2: Typical particle size distributions for a series of magnalium samples of different particle sizes used to study the influence of particle size on the strobe frequency.

3. Results:

The high-speed camera movies reveal details on the process involved (see Figure 3). A qualitative analysis shows that the frequency of flashes increases with decreasing particle size of magnalium and with increasing magnalium weight percentage. Initially, when the pellet is ignited, a layer appears on the top of the pellet. The surface is heated up by a reaction, becomes red and white hot spots develop on the surface (see Figure 3(G)). For compositions with a lower frequency, the reaction proceeds for a longer time. As a result, the thickness of the layer is higher and the red colour brighter. When the flash is imminent, parts of the surface layer are ejected (flying particle Figure 3(H)) indicating the formation and rapid expansion of gas below the surface. A bright flash of several milliseconds follows after which the process is repeated. The pellet is consumed almost linearly, layer by layer.

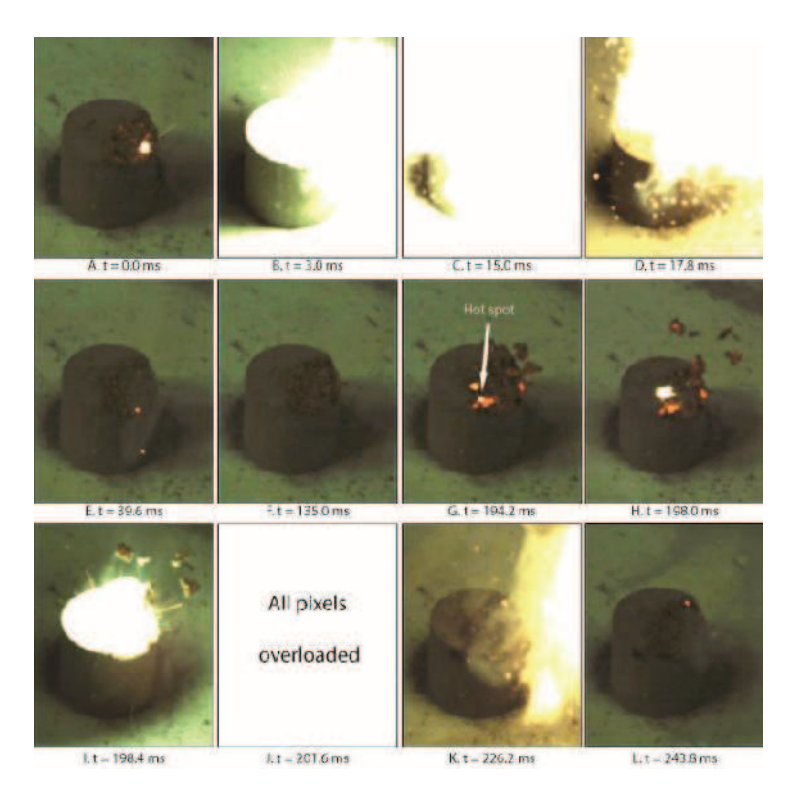


Figure 3: Series of images recorded around two flashes for a strobe composition containing 23% of magnalium (average particle size 41 μ m) recorded with a high-speed camera. Times relative to the first image are indicated under the images.

The data recorded with the photodiodes was analyzed and the frequencies were determined from the graphs using a Matlab program that calculates the mean time interval between two successive flashes. Some typical graphs are presented in Figure 4 and Figure 5 for strobes with different magnalium particle sizes (Figure 4) and different magnalium content (Figure 5). The results are summarized in Table 4 and Table 5. The strobe frequency decreases with the particle size of magnalium, in agreement with the observations made from the movies.

	Average particle size (µm)	Average of the mean time intervals (s)	Average frequency (Hz)
Composition 1.1	24,85	0.036	27,7
Composition 1.2	41,29	0.095	10,5
Composition 1.3	58,82	0.282	3.5
Composition 1.4	60,31	0.243	4,1
Composition 1.5	96,50	1.156	1,6
Composition 1.6	114.52	1.26	0.8

Table 4: Relation between particle size and strobe frequency for six strobe compositions with different particle sizes. Results are obtained from the time dependence of the emission intensity recorded with photodiodes for different spectral regions. No differences were observed for the various spectral regions. The average of the mean time interval is obtained by averaging the mean time intervals calculated for the three measurements of one composition. The average frequency is obtained by the same way.

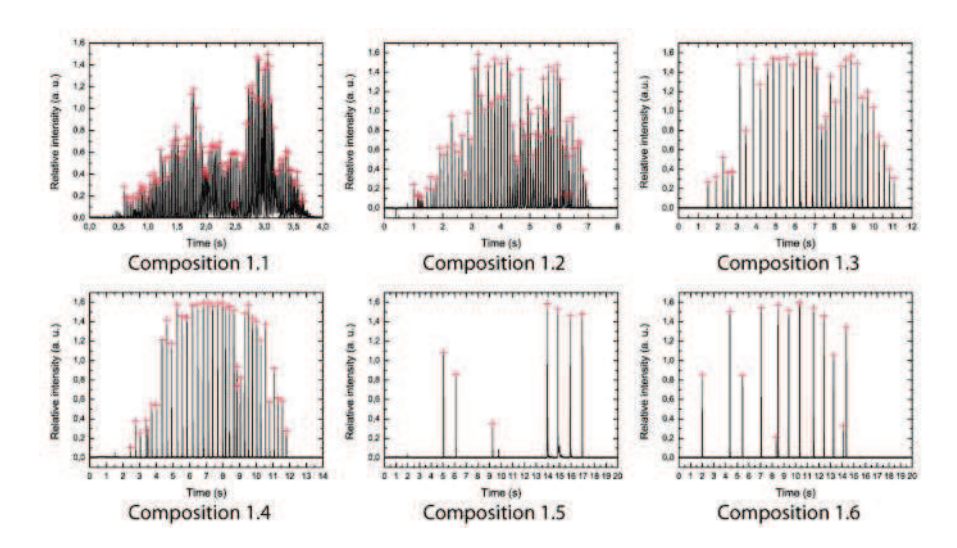


Figure 4: Temporal evolution of the intensity of the light emission for compositions with different magnalium particle sizes recorded with the photodiode sensitive in the blue spectral region. The same results are obtained for the other spectral regions.

	Magnalium content (% by weight)	Average of the mean time intervals (s)	Average frequency (Hz)
Composition 2.1	10	0.400	2,5
Composition 2.2	15	0.195	5,2
Composition 2.3	20	0.114	8,9
Composition 2.0	23	0.105	9,6
Composition 2.4	25	0.083	12,1
Composition 2.5	30	0.062	16,2
Composition 2.6	35	0.051	19,6
Composition 2.7	40	0.045	22,7
Composition 2.8	45	0.038	26,4

Table 5: Relation between particle size and strobe frequency for eight strobe compositions with different magnalium content. Results are obtained from the time dependence of the emission intensity recorded with photodiodes for different spectral regions. No differences were observed for the various spectral regions. The average of the mean time interval is obtained by averaging the mean time intervals calculated for the three measurements for one composition. The average frequency is obtained by the same way.

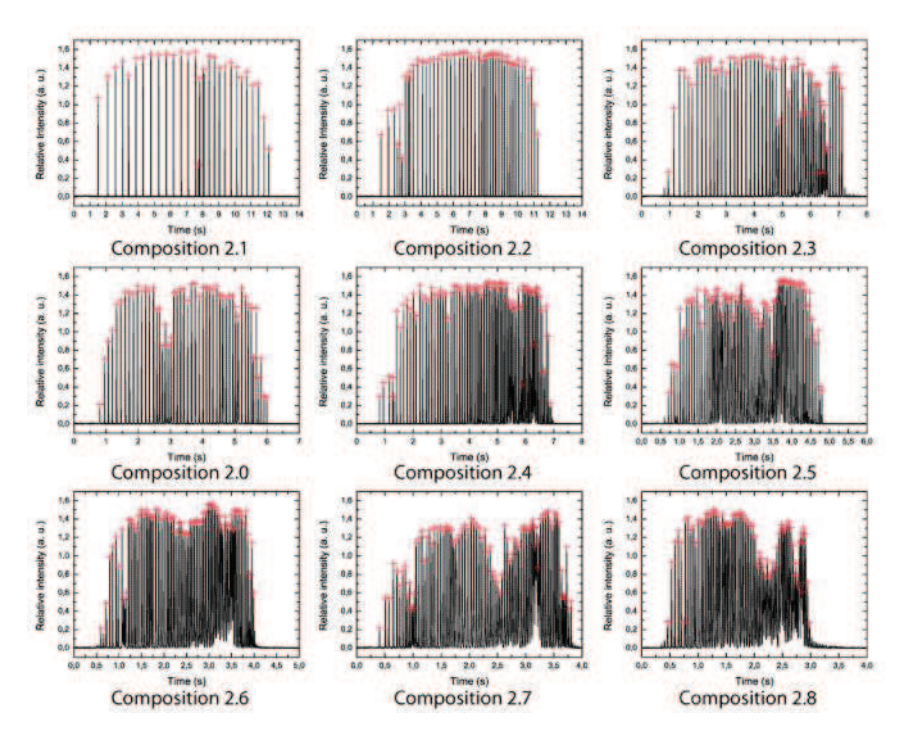


Figure 5: Temporal evolution of the intensity of the light emission for compositions with different magnalium content recorded with the photodiode sensitive in the blue spectral region. The same results are obtained for the other spectral regions.

The time intervals between two successive flashes were calculated for each composition from the data obtained with the photodiodes. The evolution of those intervals with time is shown in Figure 6 and Figure 7. It is an indicator of the regularity of the flashes and also the sharpness of the flashes. If the flashes are regular, the time intervals between two successive flashes must be constant. The tendency observed for all compositions is a decrease of the time intervals with time indicating an acceleration of the reaction. Moreover, when the strobe is fast (small average particle size and high magnalium percentage), the flashes are less sharp. On the contrary, when the strobe is slow (for high average particle size and low magnalium percentage), the flashes are less regular.

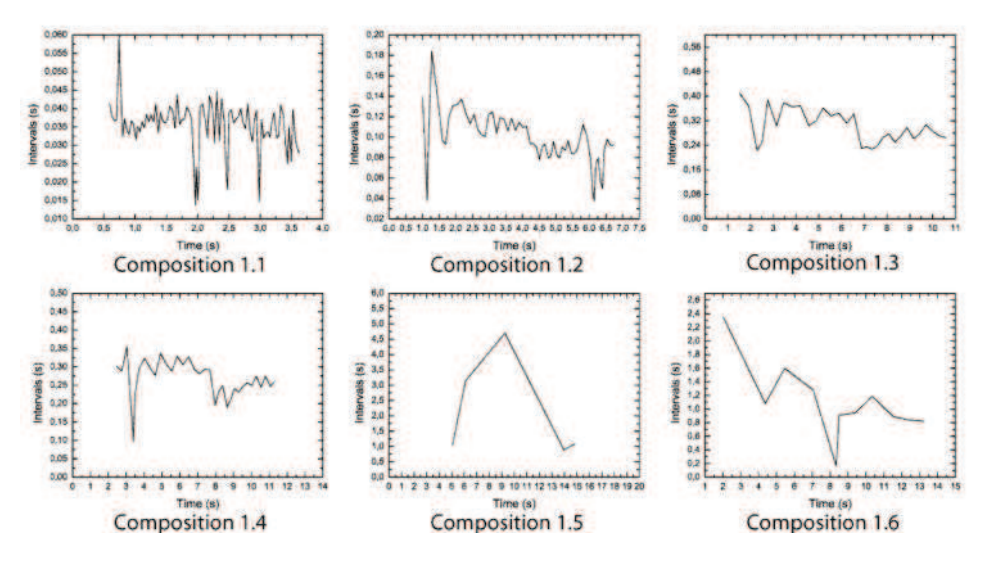


Figure 6: Evolution of the time intervals between two successive flashes for strobe compositions with different magnalium particle sizes (see Table 3 for particle sizes).

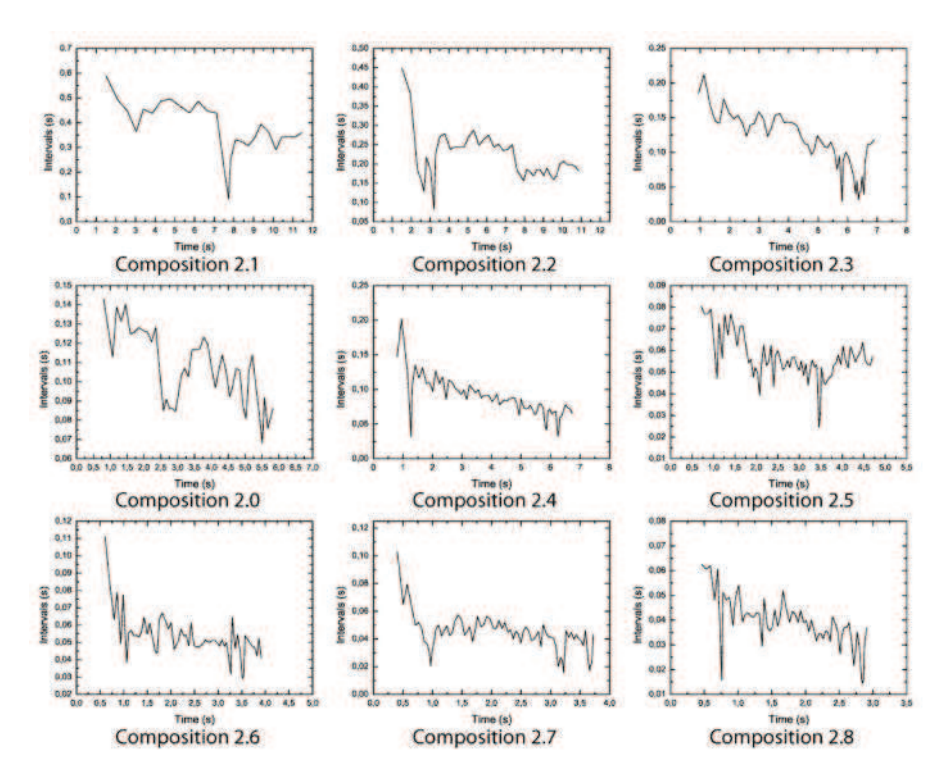


Figure 7: Evolution of the time intervals between two successive flashes for strobe compositions with different magnalium content (see Table 2 for compositions).

The mean time intervals were analyzed as a function of magnalium particle size (Figure 8(A)) and magnalium content (Figure 8(B)). The time intervals between flashes increase with particle size and decrease with higher magnalium content. Using the data, it is possible to create a strobe with any desired frequency between 1 and 30 Hz. For example, a composition containing 24% magnalium with a particle size of 41 μ m gives a strobe flashing at 12 Hz.

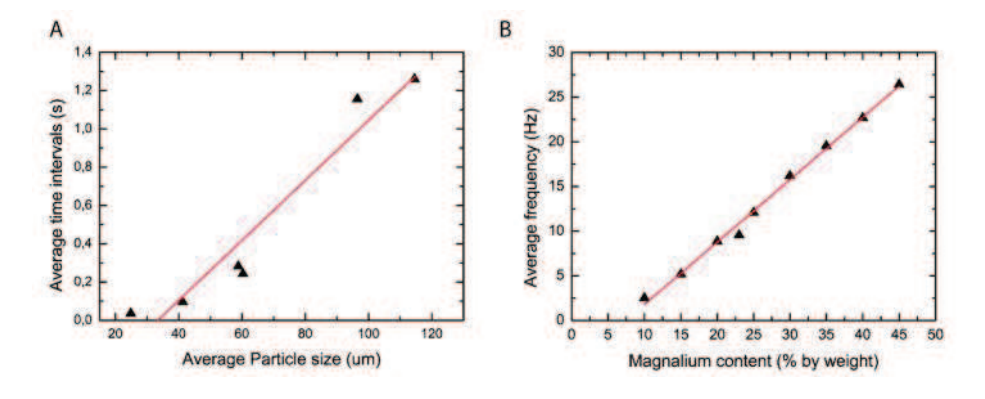


Figure 8: (A) Variation of the average time interval between flashes with magnalium particle size for the composition with 23 % magnalium. (B) Increase of the flash frequency with the magnalium content in a strobe composition with 41 μ m magnalium particles.

4. Discussion:

Strobe reactions present similarities with another kind of heterogeneous solid phase combustion, also considered as a pyrotechnic phenomenon; the Self-propagating High Temperature synthesis (SHS). They are mostly binary compositions in which when ignited, the combustion front propagates through the powdered ingredients leaving a metallic alloy or a high quality ceramic material. Spatial oscillations or laminated structures (periodic structure perpendicular to the combustion front) may be observed on the produced material due to periodic variations of the flame front velocity. Unlike strobes, this is not a desired effect and extensive studies have been conducted to understand this phenomenon (13, 22-25). The occurrence of oscillation appears to be dependent on the porosity/ density of the sample, its diameter, the particle size and shape of the reactants, dilution with a reactant or an inert material, etc. All those parameters are related to the thermal conductivity of the compositions. The assumption was made that the sample burns in layers. This implies that the characteristic time of reaction is much smaller than the time for heat transfer from one layer to the other. The heat of reaction released by an exothermic reaction in the first layer increases the temperature and the reaction rate. Assuming a low thermal conductivity most of the energy is dissipated and the second layer is slowly ignited. When all the reactants are consumed in the first layer, the reaction only begins in the next layer decreasing the front propagation velocity. A similar layer-by-layer burning is observed in the strobe combustion. Moreover, hot spots, also called scintillations in SHS studies, occur on the surface combustion of both types of compositions (SHS and strobes). They randomly arise on the surface, some tarnish and dissipate, other initiate the reaction in the neighboring areas, leading to the propagation of the reaction in the layer. The hypothesis is that thermal heterogeneities coincide with the reaction media microstructure such as molten areas. This induces a rapid acceleration of the reaction.

Based on those observations, a model is created to explain the oscillating behavior of strobe reactions. It is schematically depicted in Figure 9. The first layer containing magnalium particles is ignited, initiating burning of magnalium to magnesium oxide and aluminum oxide, a thermally activated exothermic reaction. As the temperature rises due to the reaction heat, the reaction rate increases causing an avalanche reaction culminating in a flash of light. Emission spectra taken during the flash show black body radiation and emission from electronically excited reaction products, including MgO and AlO species. Heat transfer to the next lower layer initiates an avalanche reaction in this layer and depending on the balance between heat production and heat diffusion resulting in an oscillatory flash behavior.

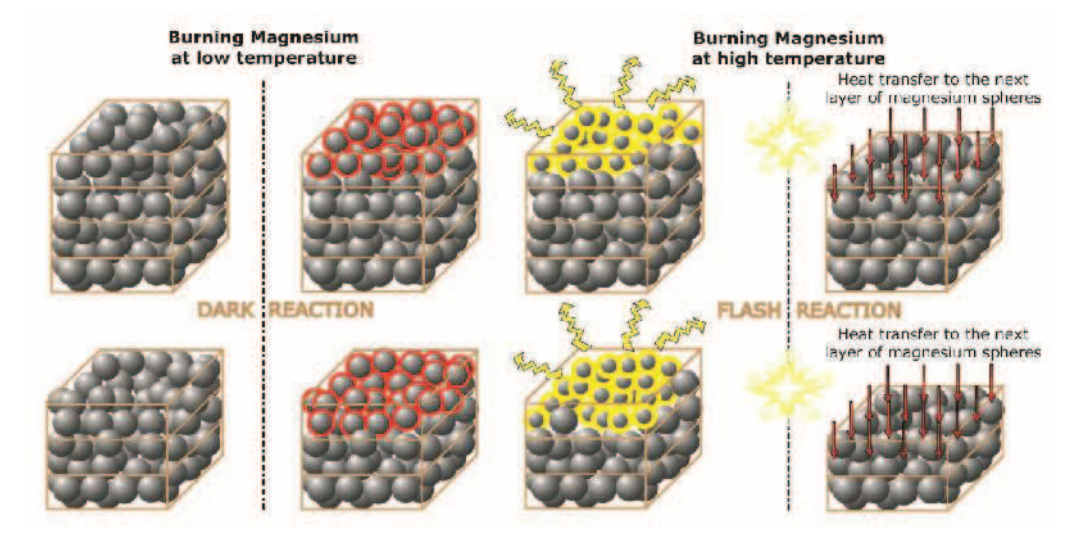


Figure 9: Schematic representation of the strobe reaction. The top left shows a strobe composed of (four) layers. The spheres are magnalium particles that start burning after igniting the top layer. During the reaction heat is produced and the reaction rate increases. This induces an avalanche reaction in which the temperature rises until all material has reacted. A short flash of light is produced due to the high temperature (black body radiation) and excited species are produced during the reaction. Part of

the reaction heat diffuses to the second layer and initiates an avalanche reaction in this layer as shown in the bottom part. The process continues until all layers have been consumed.

A detailed mathematical description of the model is based on a reaction of spheres where the change in volume is proportional to the surface area and the reaction rate increases exponentially with temperature (thermally activated reaction). The heat produced in the reaction is partly used to heat the magnalium particles and partly transferred to the surroundings. The strobe behavior model described in this paper is based on a set of non-linear coupled differential equations describing each layer. The strobe burns layer by layer as shown in Figure 9. A layer n gains heat from layer n-l, produces heat from a chemical reaction, heats the particles in it and transfers heat to n+l(See Mathematical description of the strobe behavior model in the appendix). The particle radius in layer n is then described by (Eq. 2):

$$\frac{d\binom{r_n}{r_0}}{d(\tau)} = \exp\left(-\frac{k_1}{T_n}\right)$$
 Eq. 2

Where the subscript n refers to the layer n with particle radius r_n and T_n is the dimensionless particle temperature (T of the layer n divided by 300 K). The change in temperature is given by (Eq. 3):

$$\frac{dT_n}{d\tau} = \frac{k_2}{\binom{r}{r_0}} \exp\left(-\frac{k_1}{T_n}\right) - \frac{k_3}{\binom{r_n}{r_0}} (T_n - T_{n+1}) + \frac{k_3}{\binom{r_n}{r_0}} (T_{n-1} - T_n)$$
 Eq. 3

The first term describes the heat produced by the chemical reaction, the second term the heat loss from layer n+1 and the last term the gain of heat from layer n-1.

The model uses five parameters k_1 , k_2 , k_3 , $T_{\rm ambient}$ and T_1 . The definitions for k_1 , k_2 and k_3 are provided in Table 6. $T_{\rm ambient}$ is 300 K and ignition temperature for the first layer T_1 is taken as 5, corresponding to 1500 K. This temperature is slightly lower than the maximum temperature of the flame from a butane burner that is used for igniting the strobe. The two coupled differential equations are used to model the temperature evolution in each layer n under the following boundary conditions:

- The first layer is assumed to transfer heat to only the second layer, so its temperature change is given by:

$$\frac{dT_1}{d\tau} = \frac{k_2}{\binom{r_1}{r_0}} \exp\left(-\frac{k_1}{T_1}\right) - \frac{k_3}{\binom{r_1}{r_0}} (T_1 - T_2)$$
Eq. 4

- The last layer (N) is taken to be an inert medium, which only accepts heat from the layer above it. So its temperature is determined by:

$$\frac{dT_N}{d\tau} = k_3 (T_{N-1} - T_N)$$
 Eq. 5

- At t = 0 all relative radii (r_n/r_0) are equal to 1. The temperatures of all layers except the first are the same and equal to T_{ambient} .
- As the radii decrease in the course of time they may become zero and even negative. To prevent negative radii it is postulated that, as the relative radius in any layer becomes zero, the layer does not exist anymore and the layer below it only produces heat by its chemical reaction and loses heat to the layer below it.

- The maximum temperature that can be reached is 2700 K because it is the boiling point of aluminium. It corresponds to $T = 9 (2700/T_{\rm ambient})$ and at this temperature no particles are present anymore and the layer has disappeared.

Parameter name	Formula	Description
k ₁	$\frac{E_{act}}{RT_{ambient}}$	Activation energy of the reaction divided by the gas constant and ambient temperature.
k ₂	$\frac{Q}{c_p T_{ambient}}$	Heat generated in the chemical reaction divided by the specific heat and room temperature.
k_3		Proportional to heat transfer between adjacent layers

Table 6: Description of the parameters used in the model to describe the evolution in temperature for different layers in a homogeneous composition of a strobe medium consisting of oxidizer and fuel particles.

In the modeling, values based on literature data have been used to estimate the parameters. k_1 was varied from 10 to 15 which corresponds to activation energies between 25 and 37.5 kJ/mole. Reliable numbers for the activation energy of Mg or Al oxidation are not available in literature, however a high activation energy is necessary to ensure that the reaction does not occur at ambient temperature, but can be initiated at ignition temperature T_1 . Values for k_2 can be estimated from the literature values for the standard heat of formation Q and heat capacity c_p which are 600 kJ/mole and 25 J/(mole.K), respectively, for Mg and 1670 kJ/mole and 24 J/(mole.K), respectively, for Al yielding values for k_2 equal to 80 (Mg) and 230 (Al). For the magnalium composite, values for k_2 will be in between these boundaries and in our simulations values for k_2 were varied between 100 and 200. The value for the parameter k_3 is difficult to estimate. The strobe consists of a highly conductive medium (magnalium) and poorly conducting salts. The heat transfer between adjacent layers is however crucial for the observation of strobe behaviour which depends on a balance between heating of the fuel particles and heat transfer to subsequent layers. The variation of k_3 in the simulations described demonstrates the sensitivity of the strobe behaviour on k_3 (heat transfer in the composition).

Figure 10 shows the temporal evolution of the temperature in 15 layers for different values of k_3 . For low values of k_3 (slow heat transport between layers) only the first layer burns. Increasing k_3 to 1.5 or 2.5 produces the experimentally observed strobe effect. Faster heat transfer results in a higher strobe frequency. For k_3 =3.5 heat transfer is so efficient that no heat can built up to start the avalanche flash reaction. The model beautifully reproduces the strobe behavior and demonstrates that the present model can explain oscillating strobe behavior in a homogeneous medium consisting of a fuel and an oxidizer. Longer initial time intervals for smaller k_3 values are also consistent with experiments. Furthermore, the model quantitatively reproduces the observed size dependence of the strobe frequency. The time interval between flashes is inversely proportional to r_0 , the initial particle size radius due to the larger surface area for smaller particles for the same weight fraction. The predicted linear relation between particle size and time interval between flashes shown in Figure 10(E) is in agreement with the results in Figure 8(A). The effect of adding more magnalium is mainly on k_3 . Heat transfer becomes more efficient with the fraction of conductive metal particles. If we assume that the heat transfer parameter k_3 is proportional to the metal content, a linear increase in frequency with magnesium content is predicted (Figure 10(E)), in agreement with the observations of Figure 8(B).

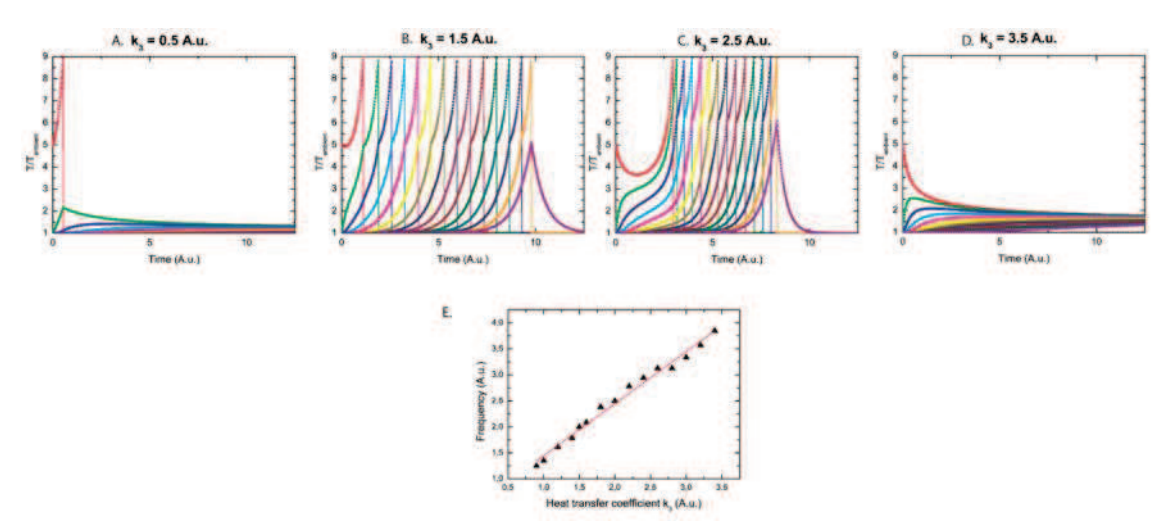


Figure 10: Graph representing the evolution of the temperature (T/T_{amb}) of magnalium particles in the successive layers for k_1 =15 and k_2 =100. The parameter k_3 , representing heat transfer between layers, is varied from 0.5 (A) to 3.5 (D). The temperature in different layers is presented by different colors from the top (red) to the bottom (purple) layer. Graph E represents the evolution of the frequency calculated from the model (in arbitrary unit) with k_3 .

In Figure 11 the strobe behavior is plotted for fixed values of k_1 and k_2 and different values for k_3 in the regime where strobe behavior is observed. In all cases the experimentally observed linear dependence is reproduced.

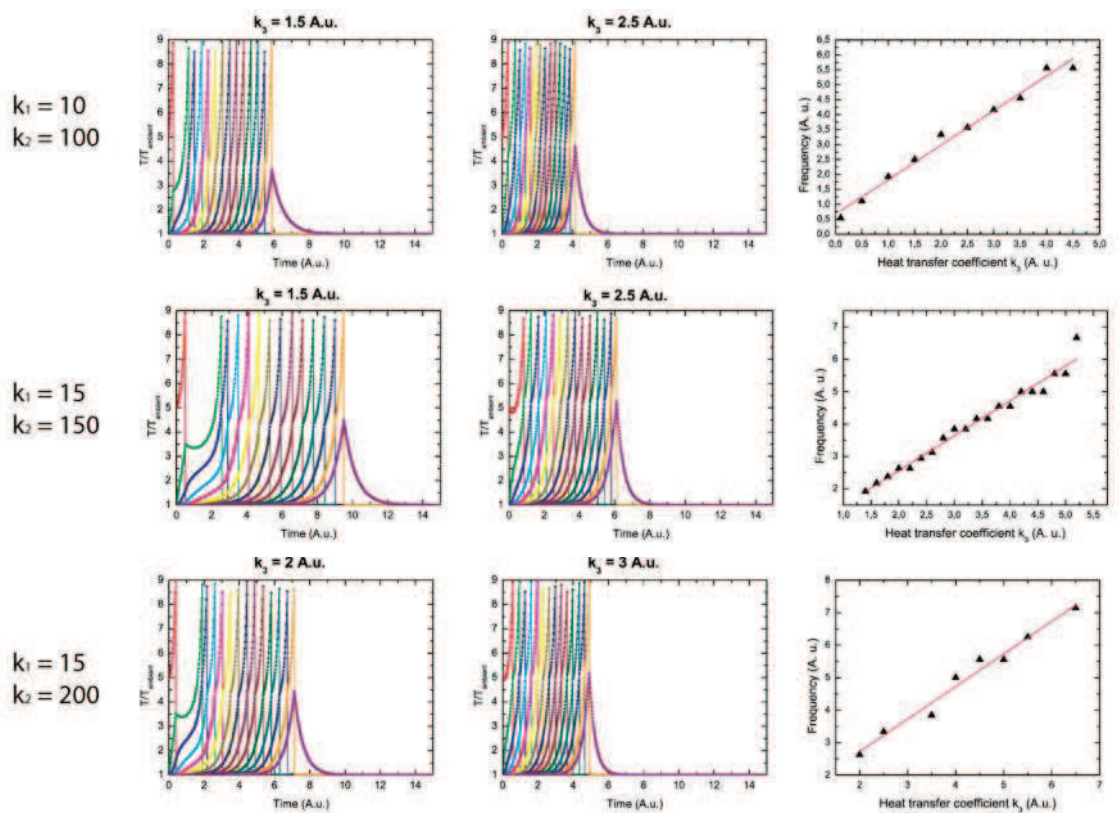


Figure 11: Relation between strobe frequency and the heat transfer coefficient k3 for $k_1=10$, $k_2=100$ (top), $k_1=15$, $k_2=150$ (middle) and $k_1=15$, $k_2=200$ (bottom). In all three panels, the two figures on the left give examples of the time evolution of the temperature for $k_3=1.5$ and $k_3=2.5$. The right-hand figure gives the frequencies determined from the simulations as a function of k_3 over a wider range.

5. Summary

A simple model is shown to accurately describe strobe behavior in pyrotechnic compositions. The model explains the observation of periodic flashes in a homogeneous medium consisting of an oxidizer and metal (fuel) particles. A good quantitative agreement is found between experimental results and the model for the relation between flash frequency and both metal particle size and content, providing strong support for the model. The present results give detailed insight into the mechanism behind the intriguing and well-known phenomenon of the brightly flashing fireworks. In addition it enables the design of strobe compositions with well-defined flash frequencies for military applications and crowd control.

Aknowledgement:

Grateful acknowledgment is given to the TNO Defense Research PhD fund for financial support and to TNO Technical Sciences for providing experimental facilities.

References:

- 1. A. I. Sidorov, I. P. Kravchenko, V. M. Antonov, N. A. Silin, P. V. Kovalenko, M. M. Arsh, patent no SU 247828 (1969 is only one reference list spanning the text, figure captions and supplementary materials.
- 2. U. Krone, patent no 2,164,437 (1973).
- 3. R. P. Cornia, patent no 3,983,816 (1976).
- 4. D. C. Sayles, patent no 4,888,464 (1989).
- 5. T. Takahashi, Y. Tsukahara, Acta Paediatrica Japonica: Overseas edition 40, 631-637 (1998).
- 6. A. S. H. Brock, Pyrotechnics: The History and Art of Fireworks Making (D. O'Connor, London, 1922).
- 7. F. Wasmann, Pyrotechnik: Grundlagen, Technologie und Anwendung, 239 (1975).
- 8. U. Krone, Pyrotechnik: Grundlagen, Technologie und Anwendung, 225 (1975).
- 9. T. Shimizu, Pyrotechnica VIII, 5 (1982).
- 10. C. Jennings-White, Journal of Pyrotechnics 20, 7 (2004).
- 11. H. P. Li, Journal of Material Research 10, 1379 (1995).
- 12. A. Makino, Progress in Energy and Combustion Science 27, 1 (2001).
- 13. A. S. Muskayan, A. S. Rogachev, Progress in Energy and Combustion Science 34, 377 (2008).
- 14. A. G. Merzhanov, I. P. Borovinskaya, Combustion, Science and technology 10, 195 (1975).
- 15. M. G. Lakshmikantha, J. A. Sekhar, Metallurgical Transactions A 24(A), 617 (1993).

- 16. H. P. Li, Chemical Engineering Science 60, 925 (2005).
- 17. V. G. Prokofiev, V. K. Smolyakov, International Journal of Self-propagating High-temperature Synthesis 15, 133 (2006).
- 18. T. Shimizu, International Pyrotechnic Seminar 16th, 47 (1991).
- 19. R. I. Grose, M. Cartwright, A. Bailey, 4, 1 (1998).
- 20. C. Feng, Q. Zeng, Z. Du, Journal of the Chemical Society, Faraday Transactions 92, 2971 (1996).
- 21. M. L. Davies, A Thermokinetic Model for the Combustion of Strobe Composition, Journal of Pyrotechnics 27, 42-49 (2008).
- 22. E. B. K. Washington, D. Aurongzeg, J. Berg, D. Osbourne, M. Holtz, M. Pantoya, International Journal of Self-propagating High-temperature Synthesis 15, 121 (2006).
- 23. J. Jung, S. Baik, Journal of the American Ceramic Society 90, 3063 (2007).
- 24. A. S. Muskayan, A. S. Rogachev, M. Mercedes, A. Varma, Chemical Engineering Science 59, 5099 (2004).
- 25. N. A. Kochetov, A. S. Rogachev, A. G. Merzhanov, Doklady Physical Chemistry 389, 80 (2003)..

Appendix:

Mathematical description of the strobe behaviour model:

To model the strobe reaction we assume a simple reaction of a spherical object for which the change in volume is proportional to the surface area where the reaction takes place. For the oxidation of the magnalium particles this gives:

$$\frac{dV}{dt} = -k \times A \times p_{o_2}$$
 Eq. (1)

where V is the volume of one particle and A its surface area, k is the rate constant of the oxidation reaction of magnalium and p_{O_2} is the oxygen pressure. We assume that the presence of oxidizer is not rate limiting and assume p_{O_2} as a constant and independent of time. By replacing V and A by their expressions as function of the radius r, equation (1) can be rewritten as:

$$\frac{dr}{dt} = -k \times p_{O_2}$$
 Eq. (2)

Thus, the radius decreases with time according to:

$$r = r_0 - kt \times p_{O_2}$$
 Eq. (3)

If the reaction rate is temperature dependent, it can be written in an Arrhenius form and the time dependence of the radius of the magnesium sphere now becomes:

$$r = r_0 - k_0 p_{O_2} \exp\left(-\frac{E_{act}}{RT'}\right) \times t$$
 Eq. (4)

The heat released by the heating of dN mol of magnesium $dQ_{heating}$ is balanced by the heat transferred to the environment dQ_{loss} so the resulting heat Q from the burning of dN mol of magnesium is:

$$Q(-dN) = dQ_{heating} + dQ_{loss}$$
 Eq. (5)

$$-QdN = c_{p}\rho VdT' + \chi A(T' - T_{ambient})dt$$
 Eq. (6)

where c_p is the specific heat of magnesium at constant pressure (J.K⁻¹.mol⁻¹), ρ is the molar density of magnesium (mol.m⁻³), V is the volume of the magnesium particle (m³), T' is the temperature of the magnesium particle (K), $T_{ambient}$ is the temperature of the atmosphere (K), χ is the heat transfer coefficient (J.K⁻¹.m⁻².s⁻¹) and A is the surface of the magnesium sphere.

Dividing Eq. (6) by dt to obtain a differential equation and by N, V and A to obtain their expressions depending on particle radius we get:

$$\frac{dT'}{dt} = -\frac{Q}{c_n \rho v r} \frac{dr}{dt} - \frac{3\chi}{c_n \rho r} (T' - T_{ambient})$$
 Eq. (7)

v being the molar volume the product ρv must equal 1.

Using the time dependence equation of the radius of magnesium sphere, the following two differential equations are obtained:

$$\frac{dT'}{dt} = \frac{k_0 p_{O_2} Q}{c_p r} \exp\left(-\frac{E_{act}}{RT'}\right) - \frac{3\chi}{c_p \rho r} (T' - T_{ambient})$$

$$\frac{dr}{dt} = -k_0 p_{O_2} \exp\left(-\frac{E_{act}}{RT'}\right)$$
Eq. (8)

The variable t is replaced by the dimensionless variable $\tau = (k_0 p_{O_2} t)/r_0$ to reach:

$$\frac{dT}{d\tau} = \frac{k_2'}{\binom{r}{r_0}} \exp\left(-\frac{k_1'}{T'}\right) - \frac{k_3}{\binom{r}{r_0}} (T' - T_{ambient})$$

$$\frac{d\binom{r}{r_0}}{d\tau} = -\exp\left(-\frac{k_1'}{T'}\right)$$
Eq. (9)

The assumption is made that the strobe burns layer by layer. The system is supposed homogeneous: particles are present in all layers in the same density. Except for the top and bottom layers, any layer n gains heat from layer n-l, produces heat from a chemical reaction, heats the particles in it and transfers heat to n+l. The relative particles radius in layer n is then described by:

$$\frac{d\binom{r_n}{r_0}}{d\tau} = \exp\left(-\frac{k_1'}{T_n'}\right)$$
 Eq. (10)

where the subscript n refers to the layer n with particle radius r_n and particle temperature T_n (it corresponds to the temperature of the layer n divided by the ambient temperature). τ is a dimensionless time, inversely proportional to the initial particle radius r_0 . The change of temperature is given by:

$$\frac{dT_{n'}}{d\tau} = \frac{k_{2'}}{\binom{r}{r_{0}}} \exp\left(-\frac{k_{1'}}{T_{n'}}\right) - \frac{k_{3}}{\binom{r_{n}}{r_{0}}} \left(T_{n'} - T_{n+1'}\right) + \frac{k_{3}}{\binom{r_{n}}{r_{0}}} \left(T_{n-1'} - T_{n'}\right)$$
Eq. (11)

The first term on the right hand size describes the heat produced by the chemical reaction. The second term on the right hand side represents the heat loss from layer n+1 and the last term the gain of heat in layer n from the layer above it, layer n-1.

A dimensionless temperature T is defined by $T'/T_{ambient}$ so parameters k_{l} and k_{2} are replaced by $k_{2} = E_{act}/RT_{ambient}$ and $k_{3} = Q/c_{p}T_{ambient}$ respectively. The two coupled differential equations obtained are:

$$\frac{dT_n}{d\tau} = \frac{k_2}{\binom{r}{r_0}} \exp\left(-\frac{k_1}{T_n}\right) - \frac{k_3}{\binom{r}{r_0}} (T_n - T_{n+1}) + \frac{k_3}{\binom{r}{r_0}} (T_{n-1} - T_n)$$

$$\frac{d\binom{r}{r_0}}{d\tau} = -\exp\left(-\frac{k_1}{T_n}\right)$$
Eq. (12)